

## Iron(III)–Salen Complexes as Enzyme Models: Mechanistic Study of Oxo(salen)iron Complexes Oxygenation of Organic Sulfides

Veluchamy Kamaraj Sivasubramanian, Muniyandi Ganesan, Seenivasan Rajagopal,\* and Ramasamy Ramaraj\*

School of Chemistry, Madurai Kamaraj University, Madurai-625 021, India

seenirajan@yahoo.com

Received August 27, 2001

The oxidation of a series of *para*-substituted phenyl methyl sulfides was carried out with several oxo(salen)iron (salen = *N,N*-bis(salicylidine)ethylenediaminato) complexes in acetonitrile. The oxo complex  $[\text{O}=\text{Fe}^{\text{IV}}(\text{salen})]^{+}$ , generated from an iron(III)–salen complex and iodosylbenzene, effectively oxidizes the organic sulfides to the corresponding sulfoxides. The formation of  $[\text{O}=\text{Fe}^{\text{IV}}(\text{salen})]^{+}$  as the active oxidant is supported by resonance Raman studies. The kinetic data indicate that the reaction is first-order in the oxidant and fractional-order with respect to sulfide. The observed saturation kinetics of the reaction and spectral data indicate that the substrate binds to the oxidant before the rate-controlling step. The rate constant ( $k$ ) values for the product formation step determined using Michaelis–Menten kinetics correlate well with Hammett  $\sigma$  constants, giving reaction constant ( $\rho$ ) values in the range of  $-0.65$  to  $-1.54$  for different oxo(salen)iron complexes. The log  $k$  values observed in the oxidation of each aryl methyl sulfide by substituted oxo(salen)iron complexes also correlate with Hammett  $\sigma$  constants, giving positive  $\rho$  values. The substituent effect, UV–vis absorption, and EPR spectral studies indicate oxygen atom transfer from the oxidant to the substrate in the rate-determining step.

### Introduction

Heme enzymes peroxidases, catalases, and cytochrome P450s are present in most organisms, and they catalyze a large variety of reactions such as oxidation, reduction, and isomerization.<sup>1–14</sup> Horseradish peroxidase (HRP) is a hemoprotein peroxidase capable of catalyzing the oxidation of a large variety of organic compounds. The

catalytic turnover of HRP involves reaction of the enzymes with  $\text{H}_2\text{O}_2$  to give a ferryl ( $\text{Fe}^{\text{IV}}=\text{O}$ ) porphyrin radical cation, two oxidation equivalents above the resting ferric state. This intermediate, known as compound **I**, is normally reduced by sequential one-electron transfers from different substrate molecules. The first of these electrons reduces compound **I** and gives compound **II**, an intermediate that is one oxidation equivalent above the ferric state. Catalytic turnover of cytochrome P450 monooxygenases require two-electron reduction of molecular oxygen to a species that is thought to resemble compound **I** of HRP, although it is not known if the second oxidation equivalent resides on the porphyrin or the protein. Despite the probable similarities in catalytic species, cytochrome P450 differs from HRP in that it routinely catalyzes the two-electron insertion of an oxygen atom into its substrates rather than the removal of a second electron.

To elucidate the mechanism of reactions catalyzed by hemoproteins, cytochrome P450, and peroxidases, the sulfoxidation of sulfides is a subject of current interest.<sup>13,15</sup> It has been established that, in the HRP-catalyzed sulfoxidation, the reaction is initiated by the transfer of one electron from the sulfide to the iron(IV) oxo porphyrin radical cation,  $[\text{Por}^{\bullet+}-\text{Fe}^{\text{IV}}=\text{O}]$ , which is suggested to be the active species in these reactions. The sulfoxide is then formed by the reaction of the radical cation with  $\text{Por}-\text{Fe}^{\text{IV}}=\text{O}$  (Scheme 1).

Though this mechanism holds in the HRP-catalyzed reaction, the situation is not clear on the mechanism of cytochrome P-450 oxidation of organic sulfides. Though

\* To whom correspondence should be addressed. Fax: 91-0452-859139.

(1) Ortiz de Montellano, P. R., Ed. *Cytochrome P450. Structure, Mechanism and Biochemistry*, 2nd ed.; Plenum Press: New York, 1995.

(2) (a) Dunford, H. B. In *Peroxidases in Chemistry and Biology*; Everse, J., Everse, K. E., Giishman, M. B., Eds.; CRC Press: Boca Raton, FL, 1991; Vol. II, pp 1–24. (b) Dunford, H. B.; Stillman, J. S. *Coord. Chem. Rev.* **1987**, *19*, 187.

(3) (a) Watanabe, Y.; Groves, J. T. In *The Enzyme*; Sigman, D. S., Ed.; Academic Press: San Diego, CA, 1992; Vol. XX, Chapter 9. (b) Bruce, T. C. In *Mechanistic Principles of Enzyme Activity*; Liebman, F. F., Greenberg, A., Eds.; VCH: New York, 1988; p 227.

(4) (a) *Metalloporphyrins in Catalytic Oxidations*; Sheldon, R. A., Ed.; Marcel Dekker: New York, 1994. (b) *Metalloporphyrins Catalyzed Oxidation*; Montanari, F., Casella, L., Eds.; Kluwer Academic Publishers: Dordrecht, The Netherlands, 1994.

(5) Meunier, B., Ed. *Biomimetic Oxidations Catalyzed by Transition Metal Complexes*; Imperial College Press: London, 2000.

(6) (a) Que, L., Jr.; Ho, R. Y. N. *Chem. Rev.* **1996**, *96*, 2607. (b) Holm, R. H. *Chem. Rev.* **1987**, *87*, 1401.

(7) (a) Sono, M.; Roach, M. P.; Coulter, E. D.; Dawson, J. H. *Chem. Rev.* **1996**, *96*, 2841. (b) Dawson, J. H. *Science* **1988**, *240*, 433.

(8) Meunier, B. *Chem. Rev.* **1992**, *92*, 1411.

(9) Feig, A.I.; Lippard, S. J. *Chem. Rev.* **1994**, *94*, 259.

(10) Brothers, P. J. In *Advances in Organometallic Chemistry*; Stone, F. G. A., West, R., Eds.; Academic Press: New York, 2001; Vol. 46, p 264.

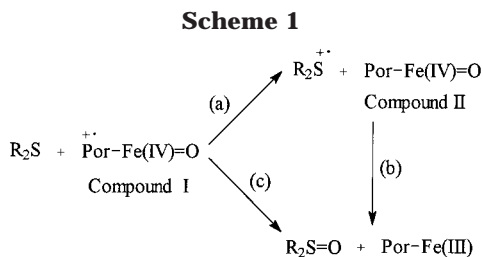
(11) Mansuy, D. *Coord. Chem. Rev.* **1993**, *125*, 129.

(12) Nam, W.; Han, H. J.; Oh, S. Y.; Lee, Y. J.; Choi, M. H.; Han, S. Y.; Kim, C.; Woo, S. K.; Shin, W. *J. Am. Chem. Soc.* **2000**, *122*, 8677.

(13) Goto, Y.; Matsui, T.; Ozaki, S.; Watanabe, Y.; Fukuzumi, S. *J. Am. Chem. Soc.* **1999**, *121*, 9497.

(14) (a) Groves, J. T.; Nemo, T. E. *J. Am. Chem. Soc.* **1983**, *105*, 5786. (b) Groves, J. T.; Subramanian, D. V. *J. Am. Chem. Soc.* **1986**, *106*, 2177. (c) Groves, J. T. *J. Chem. Educ.* **1985**, *62*, 928.

(15) (a) Ozaki, S.-I.; Ortiz de Montellano, P. R. *J. Am. Chem. Soc.* **1994**, *116*, 4487. (b) Ozaki, S.-I.; Ortiz de Montellano, P. R. *J. Am. Chem. Soc.* **1995**, *117*, 7056.



an electron-transfer mechanism is possible, also viable is a direct oxygen-transfer mechanism from the  $\text{Por}^{\text{IV}}=\text{O}$  to sulfide as shown in Scheme 1, path c.

To establish the nature of the reactive intermediate and the mechanism of cytochrome P450-catalyzed oxidation of biological substrates, extensive studies have been made using synthetic model iron–porphyrins in different oxidation states and with various ligands with the aid of spectroscopic techniques including electronic absorption, NMR, EPR, and resonance Raman (RR).<sup>13–32</sup> Interestingly no attempt has been made so far on the use of iron(III)–salen complexes as catalysts for the oxidation of biologically important organic substrates, particularly sulfides.

Salicylidene-ethylenediamines, commonly known as salens, can form stable complexes with transition metals. Apart from the porphyrins, the most important synthetic ligand systems, especially in the context of catalysis for the asymmetric oxidation of organic substrates, are the salens,<sup>33,34</sup> since metal–salen complexes have features in common with metalloporphyrins with respect to their structure and catalytic activity. These metal–Schiff base complexes have been developed as catalysts for the epoxidation of olefins and oxidation of other organic substrates, and a breakthrough has been made with this

type of salen complex in the epoxidation of simple olefins.<sup>33,34</sup> It is possible to introduce chiral substituents at C3 and C3' sites of the phenolic part of the salen ligand (cf. eq 1 for the structure of iron–salen complexes). These stereogenic carbon atoms reside proximate to the metal center, and this renders the salen ligand a promising chiral template for the construction of an asymmetric reaction site. To understand the mechanism of oxygen transfer from oxometal ions, for example, oxometal porphyrin and oxo(salen)metal complexes, organic sulfides seem to be better substrates than olefins because of the efficient reactivities of sulfides and absence of other undesired reactions.<sup>13</sup>

With the aim of establishing the optimum conditions for the synthesis of organic sulfoxides and the mechanism of oxometal ion oxidation of organic sulfides, we have initiated a systematic study on the kinetics of oxo(salen)–metal ion oxidation of the above substrates and already reported the mechanism of oxo(salen)manganese(V),<sup>35–37</sup> oxo(salen)chromium(V),<sup>38</sup> and oxo(salen)ruthenium(V)<sup>39</sup> oxygenation of organic sulfides. We have initially proposed single electron transfer from organic sulfide to the oxometal ion as the rate-controlling step in the oxygen atom transfer reaction from several cationic oxo(salen)–manganese(V)<sup>35</sup> complexes to sulfide. However, in a subsequent study, by comparing the reactivity of organic sulfides and sulfoxides toward the same oxidant, oxo(salen)manganese(V), a common mechanism involving the electrophilic attack of the oxygen of the oxidant at the sulfur center of the substrate has been proposed.<sup>37</sup> Similarly, the selective oxidation of organic sulfides to sulfoxides with oxo(salen)chromium(V) complexes proceeds through the electrophilic attack of oxygen at the sulfur center of the organic sulfide.<sup>38</sup>

The oxygenation reaction of organic sulfides with oxo(salen)manganese(V) and oxo(salen)chromium(V) ions proceeds through clear second-order kinetics, first-order each in the oxidant and substrate, and there is no precoordination between the substrate and catalyst during the course of reaction. Enzyme-catalyzed reactions achieve high enantioselectivity, at least in part, by inducing substrate precoordination to the catalyst prior to reaction.<sup>40</sup> The precoordination minimizes the degrees of freedom in the critical transition state and maximizes the selectivity-determining interactions between the catalyst's asymmetric environment and the substrate. Many successful nonenzymatic asymmetric catalyst systems operate on this principle, though a number of exceptions have also been reported.<sup>41–44</sup>

- (16) Fujii, H. *J. Am. Chem. Soc.* **1993**, *115*, 4641.  
 (17) Traylor, P. S.; Kim, C.; Richards, J. L.; Xu, F.; Perrin, C. L. *J. Am. Chem. Soc.* **1995**, *117*, 3468.  
 (18) Gross, Z.; Nimri, S. *Inorg. Chem.* **1994**, *33*, 1731.  
 (19) Czarrecki, K.; Nimri, S.; Gross, Z.; Proniewicz, L. M.; Kincaid, J. R. *J. Am. Chem. Soc.* **1996**, *118*, 2929.  
 (20) Ohta, T.; Matsuura, K.; Yoshizawa, K.; Morishima, I. *J. Inorg. Biochem.* **2000**, *82*, 141 and references therein.  
 (21) Vassel, K. A.; Espenson, J. H. *Inorg. Chem.* **1994**, *33*, 5491.  
 (22) (a) Guilmet, E.; Meunier, B. *Tetrahedron Lett.* **1980**, *21*, 4449.  
 (b) Guilmet, E.; Meunier, B. *Tetrahedron Lett.* **1982**, *23*, 2449.  
 (23) Oae, S.; Watanabe, Y.; Fujimori, K. *Tetrahedron Lett.* **1982**, *23*, 1189.  
 (24) (a) Smegal, J. A.; Schardt, B. C.; Hill, C. L. *J. Am. Chem. Soc.* **1983**, *105*, 3510. (b) Smegal, J. A.; Hill, C. L. *J. Am. Chem. Soc.* **1983**, *105*, 3515.  
 (25) Mansuy, D.; Bortoli, J. F.; Momenteau, M. *Tetrahedron Lett.* **1982**, *23*, 2781.  
 (26) Roach, M. P.; Pond, A. E.; Thomas, M. R.; Boxer, S. G.; Dawson, J. H. *J. Am. Chem. Soc.* **1999**, *121*, 12088.  
 (27) Candelas, L. P.; Folkes, L. K.; Wardman, P. *Biochemistry* **1997**, *36*, 7081.  
 (28) Yun, C. H.; Miller, G. P.; Guengerich, F. P. *Biochemistry* **2000**, *39*, 1139.  
 (29) (a) Sato, H.; Guengerich, J. *J. Am. Chem. Soc.* **2000**, *122*, 8099.  
 (b) Zakhariyeva, O.; Trautwein, A. X.; Veeger, C. *Biophys. Chem.* **2000**, *88*, 11 and references therein.  
 (30) Guo, C. C.; Song, J. X.; Chen, X. B.; Jiang, G. F. *J. Mol. Catal., A* **2000**, *157*, 31.  
 (31) (a) Wirstam, M.; Blomberg, M. R. A.; Siegbahn, P. E. M. *J. Am. Chem. Soc.* **1999**, *121*, 10178. (b) Moore, K. T.; Horvath, I. T.; Therien, M. J. *Inorg. Chem.* **2000**, *39*, 3125.  
 (32) Ogliaro, F.; Harris, N.; Cohen, S.; Filatov, M.; de Visser, S. P.; Shaik, S. *J. Am. Chem. Soc.* **2000**, *122*, 8977.  
 (33) (a) Canali, L.; Sherrington, D. C. *Chem. Soc. Rev.* **1999**, *28*, 85.  
 (b) Katsuki, T. *Coord. Chem. Rev.* **1995**, *140*, 189. (c) Ito, Y. N.; Katsuki, T. *Bull. Chem. Soc. Jpn.* **1999**, *72*, 603.  
 (34) Jacobsen, E. N. In *Comprehensive Organometallic Chemistry II*; Wilkinson, G., Stone, F. G. A., Abel, E. W., Hegedus, L. S., Eds.; Pergamon: New York, 1995; Vol. 12, Chapter II.1.

- (35) Chellamani, A.; Alhaji, N. M. I.; Rajagopal, S.; Sevel, R.; Srinivasan, C. *Tetrahedron* **1995**, *51*, 12677.  
 (36) Chellamani, A.; Alhaji, N. M. I.; Rajagopal, S. *J. Chem. Soc., Perkin Trans. 2* **1997**, 299.  
 (37) Chellamani, A.; Kulandaipandi, P.; Rajagopal, S. *J. Org. Chem.* **1999**, *64*, 2232.  
 (38) Sevel, R.; Rajagopal, S.; Srinivasan, C.; Alhaji, N. M. I.; Chellamani, A. *J. Org. Chem.* **2000**, *65*, 3334.  
 (39) Kulandaipandi, P. Ph.D. Thesis, Manonmaniam Sundaranar University, 1999.  
 (40) Walsh, C. *Enzymatic Reaction Mechanisms*; W. H. Freeman and Co.: New York, 1979.  
 (41) Hoveyda, A. H.; Evans, D. A.; Fu, G. C. *Chem. Rev.* **1993**, *93*, 1307.  
 (42) *Catalytic Asymmetric Synthesis*; Ojima, I., Ed.; VCH: New York, 1993.  
 (43) Kolb, H. C.; van Nieuwenhze, M. S.; Sharpless, K. B. *Chem. Rev.* **1994**, *94*, 2483.  
 (44) Palucki, M.; Finney, N. S.; Pospisil, P. J.; Guler, M. L.; Ishida, T.; Jacobsen, E. N. *J. Am. Chem. Soc.* **1998**, *120*, 948 and references therein.

**Table 1.**  $\lambda_{\max}$  Absorption, Magnetic Moment, and Electrochemical Data of Schiff Base Complexes of Iron

| complex   | magnetic moment at 300 K ( $\mu_B$ ) | $\lambda_{\max}$ (nm), <sup>a</sup> iron salen | $\lambda_{\max}$ (nm), <sup>a</sup> oxo(salen)iron | $E_{1/2}$ V (SCE) <sup>b</sup> |
|---|--------------------------------------|--|--|--------------------------------|
| [Fe(salen)Cl]   | 5.43 (5.37) <sup>c</sup>             | 470  | 450  | -0.28                          |
| [Fe(5,5'-(NO <sub>2</sub> ) <sub>2</sub> salen)Cl]    | 5.11                                 | 463  | 459  | -0.15                          |
| [Fe(5,5'-(Cl) <sub>2</sub> salen)Cl]                  | 5.19 (5.14) <sup>c</sup>             | 470  | 462  | -0.24                          |
| [Fe(5,5'-(OMe) <sub>2</sub> salen)Cl]                 | 5.61                                 | 500  | 466  | -0.35                          |
| [Fe(7,7'-(Me) <sub>2</sub> salen)Cl]                  | 5.57                                 | 468  | 461  | -0.30                          |
| [Fe(3,3',5,5'-( <i>t</i> -But) <sub>4</sub> salen)Cl] | 5.65                                 | 503  | 495  | -0.68                          |

<sup>a</sup> In 100% CH<sub>3</sub>CN at 298 K. <sup>b</sup> The supporting electrolyte is 0.1 M NaClO<sub>4</sub>. <sup>c</sup> Reported values.<sup>54</sup>

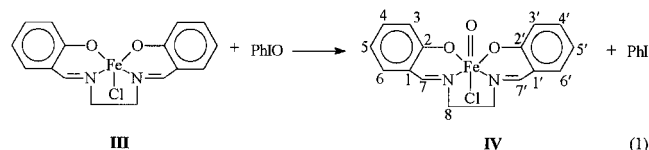
Despite the widespread interest in iron(III)–porphyrin-catalyzed oxygenation of organic sulfides,<sup>1,6,13,45–53</sup> so far no attempt has been made to use iron(III)–salen complexes as catalysts. Though salen complexes of Mn<sup>III</sup>, Cr<sup>III</sup>, Co<sup>III</sup>, Ru<sup>III</sup>, and other metal ions have been used as catalysts, it is surprising that the catalytic role of iron(III)–salen complexes has not been realized on the oxygenation reactions of organic sulfides.<sup>33–39</sup> The present study seems to be the first attempt to use oxo(salen)iron complexes as the oxidants for the sulfoxidation of organic sulfides. Interestingly the reaction proceeds through precoordination of the substrate to the oxidant, and the synthetic and mechanistic details of oxo(salen)iron complex oxygenation of organic sulfides are discussed here.

### Experimental Section

**Materials.** The iron(III)–Schiff base complexes **IIIa–IIIf** were prepared by the reaction of stoichiometric amounts of ligands with the ferric chloride in alcohol solution and recrystallized using the appropriate solvents.<sup>54–56</sup> The corresponding oxo(salen)iron complexes **IVa–IVf** were obtained by the following procedure. The stirring of a clear solution of iron(III)–salen complexes in CH<sub>3</sub>CN with iodosylbenzene (PhIO) for 5–15 min led to the formation of oxo(salen)iron species **IVa–IVf**. The structures of iron(III)–salen and oxo(salen)iron complexes used in the present study are shown in eq 1.

*p*-Methoxy- and *p*-methylphenyl thiols (Aldrich) were obtained and converted to sulfides by the known procedures.<sup>57,58</sup> *p*-Bromo-, *p*-cyano-, *p*-fluoro-, and *p*-nitrophenyl methyl sulfides (Aldrich) were used as received. The other sulfides were prepared and purified by the reported procedures.<sup>59–61</sup> All

other reagents were of AnalaR grade or were used after purification. The kinetic study of the reaction was performed after the purities of the reactants and solvents used in the system were confirmed.



**IIIa, IVa:** unsubstituted; **IIIb, IVb:** 5,5'-(NO<sub>2</sub>)<sub>2</sub>; **IIIc, IVc:** 5,5'-Cl<sub>2</sub>; **IIId, IVd:** 5,5'-(OCH<sub>3</sub>)<sub>2</sub>; **IIIe, IVe:** 7,7'-(CH<sub>3</sub>)<sub>2</sub>; **IIIf, IVf:** 3,3',5,5'-(*t*-but)<sub>4</sub>

**Methods.** The magnetic moments of the iron(III)–salen complexes were measured by the Guoy method, and the values are collected in Table 1. The magnetic moment values are in agreement with those reported.<sup>54</sup> The equipment was calibrated by means of mercury(II) tetrathiocyanatocobaltate(II). The IR spectra of the complexes were measured with a JASCO FTIR-410 spectrophotometer in CH<sub>3</sub>CN medium. The  $\nu$ (C–O) band at 1252 cm<sup>-1</sup> and  $\nu$ (H–C=N) band at 1633 cm<sup>-1</sup> were found for complex **IIIb**. Similar values were also obtained for other complexes. The EPR spectra at room temperature for complexes **IIIa** and **IIId** and their oxo forms **IVa** and **IVd** were measured with a JEOL JES-TE 100 x-band EPR spectrometer in CH<sub>3</sub>CN at room temperature. The redox potentials of complexes **IIIa–IIIf** were measured in CH<sub>3</sub>CN using an EG&G Princeton Applied Research Potentiostat/Galvanostat model 273A equipped with an *X–Y–t* recorder and are given in Table 1.

**Resonance Raman Measurements.** Resonance Raman (RR) measurements were carried out at room temperature using acetonitrile solvent with excitation of the 488 nm line of an Ar<sup>+</sup> laser (model Stabilite 2017, Spectra Physics). The excitation wavelengths match the phenolate-to-Fe charge-transfer (ArOFe CT) bands. A SPEX 1404 double monochromator with two 600-groove gratings blazed at 500 nm was used to disperse the scattered light. A liquid nitrogen cooled charge-coupled device (Princeton Instruments) with 576 × 378 pixels was used as the multichannel detector. The recorded Raman spectra were calibrated using known solvent bands as reference, and the spectral resolution is estimated as 5 cm<sup>-1</sup>. The concentration of the metal complex and the oxo form in the Raman experiments was about 1 × 10<sup>-3</sup> M. The relative Raman intensities were obtained after normalization of the spectra with the CH<sub>3</sub>CN band. The laser power of the sample was about 25–40 mW. No changes were observed in the RR spectra during the accumulation period (about 1 h), and the metal complex and the oxo species were stable throughout the experiment. This is in agreement with the observation that the absorption spectra measured before and after the RR experiments were the same.

**Kinetic Measurements.** The absorption spectra of iron(III)–salen complexes and their oxo forms were obtained using a JASCO model 7800 UV–vis spectrophotometer. The progress of the reaction was monitored spectrophotometrically by following the decay of the respective absorbance maximum of oxo complexes **IVa–IVf** at definite time intervals at 298 K. The reaction was followed up to 50% conversion. The pseudo-first-order rate constant (*k*) value for each kinetic run was

(45) (a) Kobayashi, S.; Nakano, M.; Goto, T.; Kimura, T.; Schaap, A. P. *Biochem. Biophys. Res. Commun.* **1986**, *135*, 166. (b) Kobayashi, S.; Nakano, M.; Kimura, T.; Schaap, A. P. *Biochemistry* **1987**, *26*, 5019.

(46) Doerga, D. R.; Cooray, N. M.; Brewster, M. E. *Biochemistry* **1991**, *30*, 8960.

(47) Naruta, Y.; Tani, F.; Maruyama, K. *Tetrahedron: Asymmetry* **1991**, *2*, 533; *J. Chem. Soc., Chem. Commun.* **1990**, 1378.

(48) (a) Duboc-Toia, C.; Menage, S.; Ho, R. Y. N.; Que, L., Jr.; Lambeaux, C.; Fontecave, M. *Inorg. Chem.* **1999**, *38*, 1261. (b) Duboc-Toia, C.; Menage, S.; Lambeaux, C.; Fontecave, M. *Tetrahedron Lett.* **1997**, *38*, 3727.

(49) Groves, J. T.; Viski, P. *J. Org. Chem.* **1990**, *55*, 3628.

(50) Chiang, L. C.; Konishi, K.; Aida, T.; Inoue, S. *J. Chem. Soc., Chem. Commun.* **1992**, 254.

(51) (a) Baciocchi, E.; Lanzalunga, O.; Malandrucchio, S.; Ioele, M.; Steenken, S. *J. Am. Chem. Soc.* **1996**, *118*, 8973. (b) Ioele, M.; Steenken, S.; Baciocchi, E. *J. Phys. Chem. A* **1997**, *101*, 2979.

(52) Baciocchi, E.; Lanzalunga, O.; Marconi, F. *Tetrahedron Lett.* **1994**, *35*, 9771.

(53) Baciocchi, E.; Lanzalunga, O.; Pirozzi, B. *Tetrahedron* **1997**, *53*, 12287.

(54) (a) Gerloch, M.; Lewis, J.; Mabbs, F. E.; Richards, A. *J. Chem. Soc. A* **1968**, 112. (b) Gullotti, M.; Casella, L.; Pasini, A.; Ugo, R. *J. Chem. Soc., Dalton Trans.* **1977**, 339.

(55) Gerloch, M.; Mabbs, F. E. *J. Chem. Soc. A* **1967**, 1598.

(56) Hobday, M. D.; Smith, T. D. *Coord. Chem. Rev.* **1972/73**, *9*, 311.

(57) Suter, E. M.; Hansen, H. L. *J. Am. Chem. Soc.* **1932**, *54*, 1401.

(58) Gilman, H.; Beaber, N. J. *J. Am. Chem. Soc.* **1925**, *47*, 1450.

(59) Bourgeois, M. M., Ed.; Abraham, A. *Recl. Trav. Chem. Pays-Bas* **1911**, *30*, 407.

(60) Leandri, G.; Mangini, A.; Passerine, R. *Gazz. Chim. Ital.* **1954**, *84*, 3.

(61) Burton, H.; Hu, P. F. *J. Chem. Soc.* **1946**, *68*, 498.



computed from the linear least-squares plots of  $\log(\text{absorbance})$  vs time. The rate constant for the formation of products from the oxidant–substrate complex and the Michaelis–Menten constants were evaluated using double-reciprocal plots of  $k_1$  and the concentration of the substrates.

**Product Analysis.** In a typical experiment, 0.5 mM substrate (ArSMe) was added to a 0.5 mM solution of oxo(salen)iron complex in 6 mL of solvent ( $\text{CH}_3\text{CN}$ ). The solution was stirred at 298 K for 1–3 h depending upon the nature of the sulfide and complex. At the end, the solvent was removed, and the organic product was then extracted with ether. The ether extract was dried over anhydrous  $\text{Na}_2\text{SO}_4$ , and the solvent was removed. Then the resulting residue was analyzed by IR. The IR spectrum of the product was found to be identical with that of the sulfoxide (ArSOMe), exhibiting the  $\text{S}=\text{O}$  stretching frequency in the characteristic region 1070–1030  $\text{cm}^{-1}$ . The GC analysis of the product using a model GC17A Shimadzu gas chromatograph indicated the formation of sulfoxide as the only product under the present experimental conditions. Sulfides and sulfoxides are identified by their characteristic retention times and also by co-injection with authentic samples.

## Results and Discussion

In the metal-ion-catalyzed oxygenation of organic substrates with terminal oxidants, in some reactions it has been established that the formation of oxometal species from the metal ion and the oxidant becomes the rate-determining step, thereby eluding the opportunity to understand the mechanism of more important oxygen atom transfer from oxometal ion to organic substrates.<sup>62</sup> To avoid this difficulty, in the present study, oxo(salen)-iron complexes **IVa–IVf** have been synthesized from iron(III)–salen complexes **IIIa–IIIf** and PhIO and then used for the oxygenation of organic sulfides (eq 1).

**Absorption Spectral Studies.** The parent iron(III)–salen complex shows characteristic absorption at  $\lambda_{\text{max}} = 470$  nm. This absorption maximum is sensitive to the nature of the substituent in the salen ligand. Introduction of a 5- $\text{NO}_2$  group shifts the  $\lambda_{\text{max}}$  value from 470 to 463 nm, whereas 5-OMe causes a large shift from 470 to 500 nm (Table 1). The formation of oxoiron complex **IVa** is inferred from the following experimental observations: (i) the dark color of the iron(III)–salen solution faded upon the addition of PhIO and (ii) there was a change in the shape of the spectrum and a substantial shift in the  $\lambda_{\text{max}}$  value (Table 1, Figure 1 (left)). For the parent complex,  $\lambda_{\text{max}}$  shifts from 470 to 450 nm, and in the methoxy-substituted complex,  $\lambda_{\text{max}}$  shifts from 500 to 466 nm. When the substrate methyl phenyl sulfide (MPS) is added to the oxoiron ion, a shift of 15 nm is noticed, i.e., from 450 to 465 nm (Figure 1 (left)). The spectral changes observed for complex **IVb** are shown in Figure 1 (right). Further addition of substrate to the oxoiron species increases the absorbance initially followed by a regular decrease (Figure 1 (right)).

**EPR Spectral Studies.** The EPR spectrum of **IIIc** showed a broad signal at  $g = 2.81$  and a weak signal at  $g = 2.02$  (Supporting Information Figure S1). The observation of the EPR signal confirms that the iron(III) complex is in the monomeric form in solution.<sup>48</sup> The presence of bases such as  $\text{N}_3^-$ ,  $\text{CN}^-$ , and  $\text{OH}^-$  produces a low-spin environment for iron(III). Experimental  $g$  values reported in the presence of  $\text{N}_3^-$  species are 1.72,

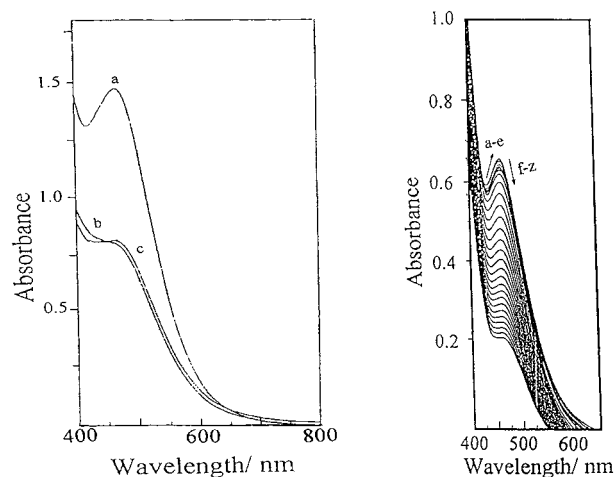


**Figure 1.** (Left) (a) Absorption spectrum of **IIIa** ( $5 \times 10^{-4}$  M) in  $\text{CH}_3\text{CN}$ . (b) Absorption spectrum of oxo(salen)iron **IVa** ( $5 \times 10^{-4}$  M). (c) Absorption spectrum after the addition of MPS to **IVa**. (Right) Absorption spectral changes (successive scans) for the oxidation of MPS ( $5 \times 10^{-3}$  M) by the oxo(salen)-iron **IVb** ( $5 \times 10^{-4}$  M) in  $\text{CH}_3\text{CN}$  (a–e are for an initial increase of absorbance, and f–z are for a decrease of absorbance with time).



**Figure 2.** (a) EPR spectrum of **IIIa**. (b) EPR spectrum of oxo(salen)iron **IVa**. (c) EPR spectrum after the addition of MPS to **IVa** in  $\text{CH}_3\text{CN}$ .

2.22, and 2.80.<sup>63,64</sup> We presume that the coordination of two phenolate ions to the iron(III) in the iron(III)–salen complexes makes the  $\text{Fe}^{\text{III}}$  state low spin, giving  $g$  values of 2.02 and 2.81. When complex **IIIc** was converted into its oxo form **IVc**, the weak signal at 2.02 disappeared and the other signal at  $g = 2.81$  was shifted to 2.53. To understand the effect of adding substrate on the EPR spectrum of the oxoiron complex, we have recorded the EPR spectrum of **IVa** in the presence of MPS. Addition of MPS to the oxo(salen)iron **IVa** resulted in the slow reappearance of the weak signal at  $g = 2.02$  (Figure 2). This observation indicates the reaction of oxo(salen)iron with the MPS, resulting in the formation of the corresponding iron(III)–salen complex. In a recent report, Yan et al.<sup>65</sup> observed similar behavior in the iron(III)–porphyrin-catalyzed hydrogen peroxide oxidation of naphthol.

**Resonance Raman Studies.** Resonance Raman studies were carried out at room temperature using excitation at 488 nm. This wavelength coincides with the phenolate-

(63) (a) Lippard, S. J.; Berg, J. M. *Principles of Bioinorganic Chemistry*; University Science Books: 1994; p 305. (b) Drago, R. S. *Physical Methods for Chemists*, 2nd ed.; Saunders College Publishing: 1992; p 582.

(64) (a) Sobolev, A. P.; Babushkin, D. E.; Talsi, E. P. *J. Mol. Catal., A* **2000**, *159*, 233. (b) Bertini, I.; Luchinat, C.; Parigi, G. *Eur. J. Inorg. Chem.* **2000**, 2473.

(65) Yan, Y.; Xiao, F. S.; Zheng, G.; Zhen, K.; Fang, C. *J. Mol. Catal., A* **2000**, *157*, 65.

(62) Finney, N. S.; Pospisil, P. J.; Chang, S.; Palucki, M.; Konsler, R. G.; Hansen, K. B.; Jacobsen, E. N. *Angew. Chem., Int. Ed. Engl.* **1997**, *36*, 1720.

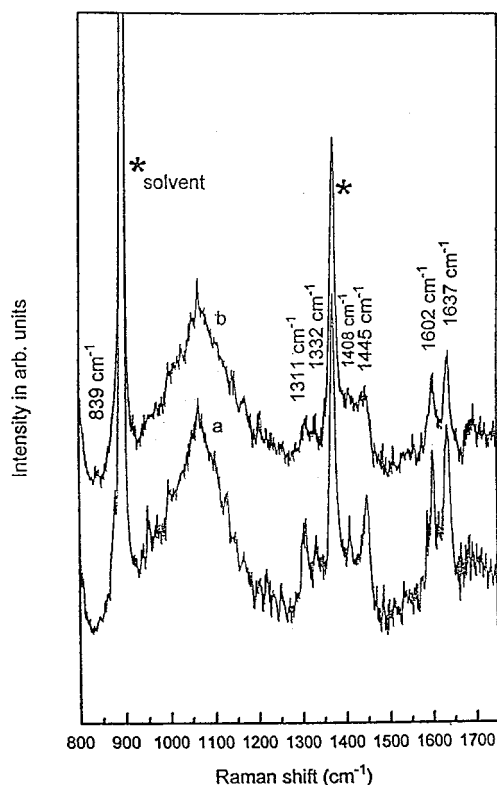


**Figure 3.** (a) Resonance Raman spectrum of **IIIa**. (b) Resonance Raman spectrum of oxo(salen)iron **IVa** in  $\text{CH}_3\text{CN}$ .

to-Fe charge-transfer ( $\text{ArO}^- \rightarrow \text{Fe CT}$ ) transition. Concerning the parent salen complex  $[\text{Fe}^{\text{III}}(\text{salen})]^+$  and its oxo complex  $[\text{O}=\text{Fe}^{\text{IV}}(\text{salen})]^+$ , the strongest RR bands are in the region between 1000 and 1700  $\text{cm}^{-1}$  (Figure 3), which includes the internal ring modes of the phenolate ligands as well as the C–O stretch vibrations.<sup>66</sup> The latter mode gives rise to a band at 1311  $\text{cm}^{-1}$ . According to previous studies on a number of ferric phenolate complexes, a frequency at 1305–1307  $\text{cm}^{-1}$  corresponds to a C–O bond length of 1.32 Å, which agrees very well with the values obtained from the crystallographic analysis of  $\text{Fe}^{\text{III}}$  complexes. Apart from the bands at 1311  $\text{cm}^{-1}$ , the RR spectrum is dominated by two more bands, one in the range 1410–1445  $\text{cm}^{-1}$  and another in the range 1600–1640  $\text{cm}^{-1}$ .

An interesting observation in the RR spectrum of the iron oxo complex compared to the  $\text{Fe}^{\text{III}}$  complex is that a dramatic decrease is observed in the intensities of all modes in the range of 1300, 1400, and 1600  $\text{cm}^{-1}$ . This behavior has previously been noted with  $\text{Fe}^{\text{III}}$ –porphyrin complexes, and the reduced intensity is characteristic of porphyrin  $\pi$ -cation formation. An additional point that has to be noted with the iron oxo complex is the appearance of a low-frequency band at 839  $\text{cm}^{-1}$ . It is interesting to recall that the low-frequency spectrum of  $[\text{O}=\text{Fe}^{\text{IV}}(\text{TMP}^+)]\text{ClO}_4$  exhibits a polarized  $\nu(\text{Fe}=\text{O})$  mode at 835  $\text{cm}^{-1}$ . Surprisingly the compound **II** analogue  $[\text{O}=\text{Fe}^{\text{IV}}(\text{TMP})]$  also has a band in this region,  $\nu(\text{Fe}=\text{O}) = 843 \text{ cm}^{-1}$ .<sup>67</sup> Thus, the low-frequency band observed in the present study at 839  $\text{cm}^{-1}$  can be taken as evidence for the formation of  $\text{O}=\text{Fe}^{\text{IV}}$  due to the

oxidation of  $\text{Fe}^{\text{III}}$  with PhIO. The decrease in intensity of all peaks in the range 1300–1700  $\text{cm}^{-1}$  may be taken as evidence for the formation of a ligand cation radical. The RR spectra of phenoxy radical–metal complexes display one prominent peak at 1505–1525  $\text{cm}^{-1}$  together with a small one at around 1590  $\text{cm}^{-1}$ . However, previous studies indicate that the phenoxy radical shows quinoid character with substantial delocalization of the unpaired electron over the respective phenyl ring. Thus, the absence of a peak at 1505–1525  $\text{cm}^{-1}$  may be due to the delocalization of the unpaired electron. Thus, on the basis of the RR spectral study, the oxo(salen)iron complex may be represented as  $[\text{O}=\text{Fe}^{\text{IV}}(\text{salen})]^+$ , similar to compound **I**.

**Electrochemical Properties of Iron(III) Complexes.** The cyclic voltammograms of all the iron(III)–salen complexes were recorded, and the reduction potential ( $E_{1/2}$ ) values in  $\text{CH}_3\text{CN}$  are collected in Table 1. It is interesting to note that the  $E_{1/2}$  value is highly sensitive to the nature of the substituent and the  $E_{1/2}$  values of iron(III) complexes with 5,5′-substituents in the salen ligand correlate well with the Hammett substituent  $\sigma$  constants (Supporting Information Figure S2). The reactivity of oxo(salen)iron complexes is in accordance with the redox potential values of iron(III) complexes (vide infra). Electron-withdrawing substituents on the salen ligand are expected to destabilize the oxo(salen)iron intermediate, making it a more reactive oxidant. On the contrary, the electron-releasing substituents are expected to stabilize the oxoiron species, attenuating its reactivity and thus forming a relatively less reactive oxidant. This can be clearly verified if the redox potentials of oxo(salen)iron complexes are measured. But our attempts to measure the redox potentials of oxoiron complexes did not succeed due to the instability of  $\text{Fe}^{\text{IV}}$  and  $\text{Fe}^{\text{V}}$  species under the electrochemical reaction conditions.

**Kinetic Results.** The kinetics of oxygenation of organic sulfides with oxo(salen)iron complexes in  $\text{CH}_3\text{CN}$  were followed under pseudo-first-order conditions in the presence of at least a 10-fold excess of substrate over the oxidant by measuring the change in the absorbance at the absorption maximum of the oxo(salen)iron complex with time at 298 K. A sample run for the oxygenation of MPS with **IVb** is shown in Figure 1 (right). The observation of an initial increase (Figure 1 (right, a–e) and shift in the absorbance followed by a regular decrease (Figure 1 (right, f–z) after the addition of sulfide to the oxidant is interesting. This may be taken as supporting evidence for the coordination of substrate to the oxidant, and the spectral changes are shown in Figure 1 (right). The initial increase in the absorbance of the oxidant due to the addition of substrate deserves comment. The shift in the  $\lambda_{\text{max}}$  value of the oxo(salen)iron complex in the presence of MPS from 450 to 465 nm indicates that the interaction between the oxidant and substrate is of charge-transfer type. It is known that organic sulfides form charge-transfer (CT) complexes with oxidants such as nitrosonium ion.<sup>68</sup> Such CT complex formation is usually too fast to observe.<sup>68</sup> In the present reaction we are able to observe the initial increase only with complex **IVb** and that too with less reactive sulfide MPS and aryl methyl sulfides carrying electron-withdrawing groups. In the presence of sulfides with electron-releasing groups and other oxo(salen)iron complexes, the complex forma-

(66) Hockertz, J.; Steenken, S.; Wieghardt, K.; Hildebrandt, P. *J. Am. Chem. Soc.* **1993**, *115*, 11222.

(67) Czarnecki, K.; Nimri, S.; Gross, Z.; Proniewicz, L. M.; Kincaid, J. R. *J. Am. Chem. Soc.* **1996**, *118*, 2929.

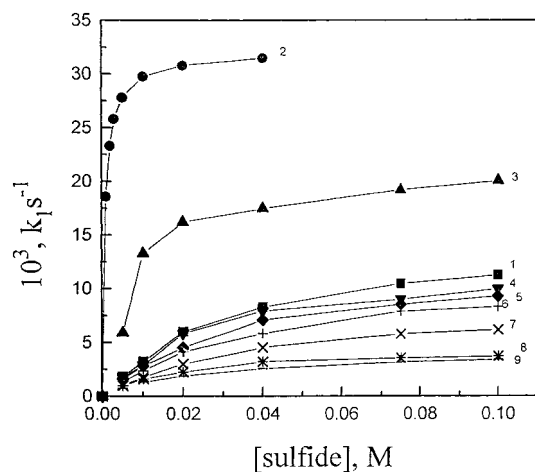
(68) Bosch, E.; Kochi, J. K. *J. Org. Chem.* **1995**, *60*, 3172.

**Table 2.** Rate Constants  $k$  and Michaelis Constants  $K_M$  Obtained from Michaelis–Menten Kinetics for Oxo(salen)iron Complexes IVa–IVf Oxidation of ArSR in CH<sub>3</sub>CN at 298 K<sup>a</sup>

| a. Rate Constants |   |                                       |              |              |              |              |              |
|-------------------|---|---------------------------------------|--------------|--------------|--------------|--------------|--------------|
| no.               | X in<br><i>p</i> -XC <sub>6</sub> H <sub>4</sub> SCH <sub>3</sub> | 10 <sup>3</sup> $k$ , s <sup>-1</sup> |              |              |              |              |              |
|                   |   | IVa                                   | IVb          | IVc          | IVd          | IVe          | IVf          |
| 1                 | H   | 4.74                                  | 17.5         | 8.91         | 0.52         | 0.63         | 0.32         |
| 2                 | OMe   | 13.3                                  | 32.1         | 20.4         | 1.13         | 1.04         | 0.82         |
| 3                 | Me  | 6.69                                  | 22.9         | 15.6         | 0.95         | 0.87         | 0.56         |
| 4                 | F   | 3.03                                  | 15.2         | 6.49         | 0.47         | 0.55         | 0.25         |
| 5                 | Cl  | 1.57                                  | 12.2         | 3.66         | 0.33         | 0.42         | 0.15         |
| 6                 | Br  | 1.46                                  | 11.5         | 2.59         | 0.30         | 0.41         | 0.12         |
| 7                 | COCH <sub>3</sub>   | 0.56                                  | 8.97         | 1.61         | 0.18         | 0.33         | 0.06         |
| 8                 | CN  | 0.49                                  | 4.49         | 1.05         | 0.13         | 0.25         | 0.03         |
| 9                 | NO <sub>2</sub>   | 0.32                                  | 4.04         | 0.84         | 0.09         | 0.21         | 0.02         |
| $\rho$            |   | -1.51 ± 0.09                          | -0.81 ± 0.05 | -1.37 ± 0.08 | -1.02 ± 0.03 | -0.65 ± 0.03 | -1.54 ± 0.05 |
| $r$               |   | 0.989                                 | 0.987        | 0.988        | 0.997        | 0.991        | 0.997        |

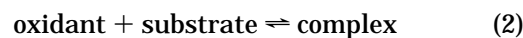
| b. Michaelis Constants |   |                       |       |      |      |      |      |
|------------------------|---|-----------------------|-------|------|------|------|------|
| no.                    | X in<br><i>p</i> -XC <sub>6</sub> H <sub>4</sub> SCH <sub>3</sub> | 10 <sup>3</sup> $K_M$ |       |      |      |      |      |
|                        |   | IVa                   | IVb   | IVc  | IVd  | IVe  | IVf  |
| 1                      | H   | 121.0                 | 42.9  | 46.7 | 26.8 | 11.8 | 14.0 |
| 2                      | OMe   | 88.1                  | 0.769 | 21.0 | 17.2 | 1.78 | 16.4 |
| 3                      | Me  | 55.7                  | 14.5  | 68.2 | 37.9 | 15.8 | 18.5 |
| 4                      | F   | 76.4                  | 38.8  | 41.8 | 26.9 | 11.3 | 9.85 |
| 5                      | Cl  | 42.1                  | 32.0  | 28.2 | 18.3 | 9.23 | 13.0 |
| 6                      | Br  | 45.9                  | 36.8  | 26.3 | 17.8 | 9.83 | 10.7 |
| 7                      | COCH <sub>3</sub>   | 20.6                  | 39.4  | 14.7 | 8.31 | 12.2 | 5.77 |
| 8                      | CN  | 30.2                  | 17.4  | 9.31 | 4.41 | 10.2 | 3.66 |
| 9                      | NO <sub>2</sub>   | 16.7                  | 21.4  | 26.9 | 2.38 | 9.04 | 6.00 |

<sup>a</sup> General conditions: [O=Fe(salen)Cl] = 5 × 10<sup>-4</sup> M.**Figure 4.**  $k_1$  vs [sulfide] for the oxidation of *p*-XC<sub>6</sub>H<sub>4</sub>SMe with IVb. The points are referred to by the same numbers as in Table 2a. [IVb] = 5 × 10<sup>-4</sup> M.

tion seems to be fast and we are not able to observe the initial increase in absorbance. Though the measurement of the equilibrium constant for the formation of an oxidant–substrate complex with the oxidant IVb and the substrates mentioned above is possible, to maintain uniformity, we did not attempt it at this stage. The nature of the complex formed between the oxidant and substrate is not known, and it requires further study, which will be taken up in the future.

The rate constant of the oxygenation reaction is measured from the decrease in absorbance with time (Figure 1 (right, f–z)). The reaction is found to be first-order in the oxidant, which is evident from the linear log-(absorbance) vs time plots. The dependence of the reaction on substrate concentration is studied by measuring the rate of the reaction at different substrate concentra-

tions, and the kinetic results are shown in Figure 4. These results indicate that the rate of the reaction increases with an increase in substrate concentration but attains saturation at high substrate concentration. The inference from this saturation kinetics is that the substrate binds to the oxidant before the rate-controlling step. Thus, the redox reaction proceeds through Michaelis–Menten kinetics (eqs 2 and 3).



On the basis of the Michaelis–Menten formulation, the observed rate constant is given by eq 4. The rearrangement of eq 4 leads to eq 5,

$$k_1 = k_{\text{obsd}} = \frac{k[\text{substrate}]}{K_M + [\text{substrate}]} \quad (4)$$

$$\frac{1}{k_1} = \frac{1}{k} + \frac{K_M}{k[\text{substrate}]} \quad (5)$$

where  $K_M$  is the Michaelis–Menten constant and  $k$  is the rate of oxidation of the substrate.

From the plot of  $1/k_1$  vs  $1/[\text{substrate}]$  (Supporting Information Figure S3) the values of  $k$  and  $K_M$  have been evaluated and collected in Table 2.

**Substituent Effects.** The sulfoxidation is highly sensitive to the nature of the substituent in the phenyl ring of phenyl methyl sulfides and in the phenolic part of the salen ligand (Table 2a). The introduction of substituents in the *para* position of the phenyl ring of phenyl methyl sulfide alters the rate appreciably; i.e., the electron-releasing substituents accelerate the rate, and the electron-withdrawing groups decelerate it. To understand the extent of charge separation in the transition



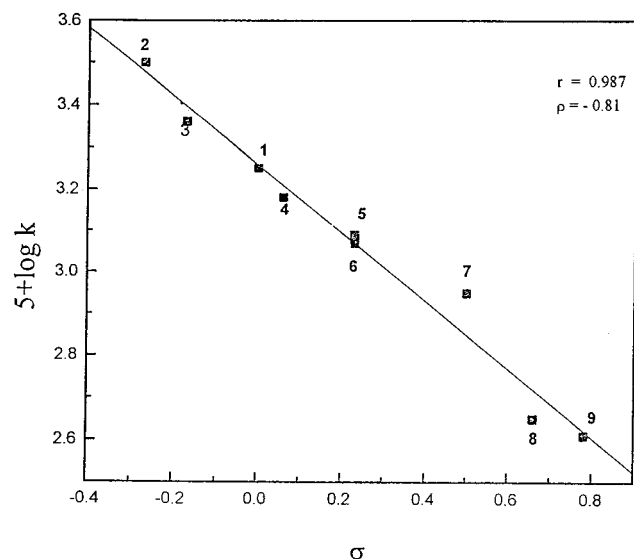


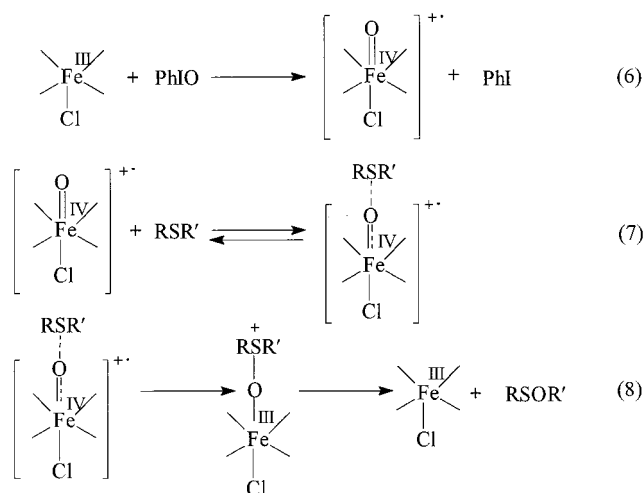
**Figure 5.** Hammett plot for the oxidation of *para*-substituted phenyl methyl sulfides with **IVb** in  $\text{CH}_3\text{CN}$  at 298 K. The points are referred to by the same numbers as in Table 2a.  $[\text{IVb}] = 5 \times 10^{-4} \text{ M}$ .

state, the  $k$  values collected in Table 2a are analyzed in terms of the Hammett equation. The correlation of  $\log k$  values of aryl methyl sulfides with the Hammett constant  $\sigma$  is good ( $r = 0.987$ ,  $n = 9$ ) (Figure 5), and the reaction constant  $\rho$  is in the range  $-0.65$  to  $-1.54$  for different oxo(salen)iron complexes. The  $\rho$  value for the reaction of sulfides with each oxo complex is given at the bottom of Table 2a. The correlation is not improved if  $\sigma^+/\sigma^-$  values are used instead of  $\sigma$  ( $r = 0.963$ ,  $n = 9$ ,  $\rho^+ = -0.45$ ) for complex **IVb**. The effect of introducing substituents in the salen ligand on the rate of reaction is also investigated (Table 2a), the observed kinetic data are also treated in terms of the Hammett equation (Supporting Information Figure S4), and the  $\rho$  value is positive ( $\rho = 0.80$ ). When we compare this  $\rho$  value with the value obtained for the  $\text{Ru}^{\text{IV}}=\text{O}$  oxidation of organic sulfides ( $\rho = 0.49$ ), we realize that the  $\rho$  value measured in the present study is higher.<sup>69</sup> An electron-transfer mechanism has been postulated for the  $\text{Ru}^{\text{IV}}=\text{O}$  oxidation of organic sulfides. It is interesting to compare the results of  $\log k$  vs  $E_{\text{ox}}$  plots (Supporting Information Figure S5) (slope  $-1.70$ ) obtained here for complex **IVb** with the recent observations made by Goto et al.<sup>13</sup> on the sulfoxidation catalyzed by high-valent intermediates of heme enzymes. They observed a slope of  $-10.5$  when the reaction proceeded through an electron-transfer mechanism and  $-2.2$  in the case of the reaction proceeding via direct oxygen transfer.

**Mechanism of the Reaction.** The experimental observations presented above can be interpreted with the mechanism shown in Scheme 2.

The observations are that (i) the reaction is fractional-order in the substrate and attains saturation kinetics at high substrate concentration and (ii) the shift in the  $\lambda_{\text{max}}$  and the initial increase in the absorbance on the addition of the substrate to the oxo(salen)iron complex indicate the formation of a complex between the oxidant and substrate. Thus, with the addition of sulfide, initial complex formation takes place via oxygen, finally leading

**Scheme 2**



to the formation of sulfoxide as shown in eqs 7 and 8. In most of the other oxidation reactions of sulfides,  $k_{\text{obsd}}$  depends linearly on the substrate concentration and no saturation kinetics is observed.<sup>13,35–38</sup> This linear dependence on substrate was taken as evidence for large  $K_M$  values (loose enzyme–substrate complexes). The saturation kinetics observed here and low  $K_M$  values (Table 2b) indicate strong binding of substrate with the oxidant. Such saturation kinetics has been observed only in some reactions involving  $\text{Fe}^{\text{III}}$ .<sup>48</sup> The  $k/K_M$  values are in the range  $0.2$ – $1.6$  with iron(III) complex **IIIb**, and these values are better than the values observed with HRP and human cytochrome P450 A12.<sup>28,70</sup>

As the iron(III)–salen complex synthesized in the present study is a five-coordinate complex carrying a chloride ion, the addition of PhIO leads to the formation of the oxo complex **IVa**, which is six-coordinate. The effect of added imidazole (Im) on the rate of the oxidation reaction also provides a clue to the mechanism of the reaction. In the presence of Im (0.05 M), the reaction is not taking place between **IVa** and MPS. This behavior of Im may be accounted for in two ways. Im forms a hydrogen bond with the oxygen of the oxo species, thus preventing the coordination of sulfide. We have already emphasized that coordination of the substrate to the oxidant is a necessary condition for the reaction to occur. Alternatively Im may lead to the formation of oxo dimer  $\text{O}[\text{Fe}(\text{salen})\text{Cl}]_2$ , which is not able to oxidize the sulfide. Thus, the effect of Im also supports direct oxygen atom transfer from the oxidant to the substrate as the mechanism of the reaction. Direct oxygen transfer from the oxidant to the substrate has been postulated in the iron(III)–porphyrin-catalyzed hydrogen peroxide oxidation of organic sulfide.<sup>71</sup> We also observe slopes of  $-1.70$  to  $-2.92$  in the plots of  $\log k$  vs  $E_{\text{ox}}$  (Supporting Information Figure S5) as observed by Goto et al.<sup>13</sup> for a reaction proceeding via direct oxygen transfer. As the reaction is carried out in cent percent  $\text{CH}_3\text{CN}$  and the rate is not influenced by the presence of oxygen, it is evident that the oxygen of the sulfoxide is only from oxo(salen)iron.

**Selective Oxidation of Sulfides to Sulfoxides.** To check the utility of this system as a useful method for

(70) Savenkova, M. I.; Kuo, J. M.; Ortiz de Montellano, P. R. *Biochemistry* **1998**, *37*, 10828.

(71) Marques, A.; di Matteo, M.; Ruasse, M. F. *Can. J. Chem.* **1998**, *76*, 770.

(69) Acquaye, J. H.; Muller, J. G.; Takeuchi, K. J. *Inorg. Chem.* **1993**, *32*, 160.

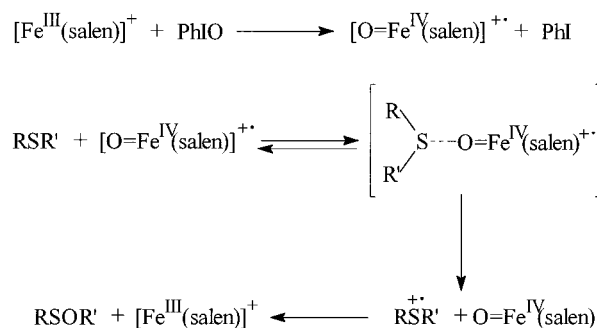
**Table 3. Selective Oxidation of *p*-XC<sub>6</sub>H<sub>4</sub>SCH<sub>3</sub> in CH<sub>3</sub>CN at 298 K by IVa and IVb<sup>a</sup>**

| X                 | IVa                 |                          | IVb                 |                          |
|-------------------|---------------------|--------------------------|---------------------|--------------------------|
|                   | reaction time (min) | % sulfoxide <sup>b</sup> | reaction time (min) | % sulfoxide <sup>b</sup> |
| H                 | 120                 | 88                       | 60                  | 100                      |
| OMe               | 90                  | 85                       | 50                  | 100                      |
| Me                | 120                 | 100                      | 60                  | 100                      |
| F                 | 120                 | 95                       | 60                  | 85                       |
| Cl                | 120                 | 78                       | 60                  | 75                       |
| Br                | 120                 | 77                       | 60                  | 68                       |
| COCH <sub>3</sub> | 120                 | 39                       | 60                  | 70                       |
| CN                | 140                 | 41                       | 80                  | 47                       |
| NO <sub>2</sub>   | 140                 | 49                       | 80                  | 45                       |

<sup>a</sup> Analyzed by GC; error limit  $\pm 5\%$ . <sup>b</sup> Only sulfides and sulfoxides are present in the reaction mixture; the difference is that of the unreacted sulfide only.

the conversion of sulfides to sulfoxides and also to confirm the mechanism of the reaction as direct oxygen atom transfer rather than electron transfer, we have measured the yield of sulfoxide formed by taking several substituted phenyl methyl sulfides and two oxidants, **IVa** and **IVb**, and the details of the percentage of sulfoxide formed are given in Table 3. The conversion of sulfide to sulfoxide is efficient and selective and depends on the nature of the substituent in the substrate and the oxidant. The high yield of sulfoxide also supports the proposed mechanism. If the reaction proceeds through an electron-transfer mechanism, the yield of sulfoxide may be low. It is pertinent to mention that Goto et al.<sup>13</sup> could get only 25% sulfoxide from the HRP compound **I** oxidation of organic sulfide when an electron-transfer mechanism was proposed and more yield when the reaction proceeded through direct oxygen transfer. A mechanism similar to this has also been proposed for the oxidation of alkanes and alkenes catalyzed with iron porphyrins.<sup>7,72</sup>

**Reactivity–Selectivity Principle.** When we compare the reactivity (rate constant values) of the four oxo(salen)iron complexes **IVa–IVd** (as the substituents are introduced in different positions in the salen ligand of complexes **IVe** and **IVf**, they are not included in this analysis) and their selectivity (the reaction constant  $\rho$ ), an interesting trend is observed, the exception being for **IVd**. Among the three complexes **IVa–IVc**, there is an inverse relationship between the reactivity and selectivity; i.e., the reactivity–selectivity principle (RSP) is applicable to this redox system. The detailed results on the application of the RSP to this redox system will be reported separately. It is worthwhile to recall that the RSP has been successfully applied to the reactions of oxo(salen)manganese(V) and oxo(salen)chromium(V) oxidation of organic sulfides and sulfoxides.<sup>36–38</sup> Thus, all these oxo(salen)metal complexes seem to proceed through a common mechanism, i.e., direct oxygen transfer from the oxidant to the substrate. The different behavior of **IVd** may indicate the operation of a different mechanism for the reaction. As this complex is least reactive among the four complexes, it should have the highest  $\rho$  value. The different behavior of **IVd** tempts us to postulate an electron-transfer mechanism for the oxidation of organic sulfides with **IVd** (Scheme 3). The change of mechanism from S<sub>N</sub>2 to electron transfer with the change in the

**Scheme 3**

reactivity of similar reactants has already been proposed in several cases.<sup>73</sup>

**Comparison with Oxo(salen)Mn<sup>V</sup>, Oxo(salen)Cr<sup>V</sup>, and Oxo(salen)Ru<sup>V</sup> Oxidations.** The oxygenation of organic sulfides with oxo(salen)metal complexes has been extensively investigated in this laboratory, and the results on oxo(salen)manganese(V),<sup>35–37</sup> oxo(salen)chromium(V),<sup>38</sup> and oxo(salen)ruthenium(V)<sup>39</sup> oxidation of sulfides have already been reported. It is worthwhile to mention the differences between the results observed in the present study and those reported earlier. The reactions with oxo(salen)chromium(V) and oxo(salen)manganese(V) complexes follow simple second-order kinetics, first-order each in the oxidant and the substrate, and the reactions involve large  $\rho$  values ( $-2.6$  with Cr<sup>V</sup> and  $-1.8$  with Mn<sup>V</sup>). To account for these results an electrophilic attack of the oxygen of the oxidant at the sulfur center of the sulfide in the rate-controlling step has been postulated. On the other hand, the results with oxo(salen)ruthenium ion oxidation of organic sulfides are similar to those of the present study; i.e., both iron and ruthenium complex oxidations proceed through saturation kinetics, i.e., Michaelis–Menten kinetics, and the  $\rho$  value ( $\rho = -0.6$  with Ru<sup>V</sup>) is low compared to that of Cr<sup>V</sup><sup>38</sup> and Mn<sup>V</sup><sup>35–37</sup> oxidations. It is pertinent to mention that the coordination of the substrate to the oxidant may facilitate chiral induction in the product if the oxidant carries a chiral center. Thus, the present redox system may be tested as a good method for the preparation of chiral sulfoxides if oxoiron complexes carrying chiral ligands are used as the oxidants. Several chiral oxo(salen)manganese(V) complexes have successfully been used for the synthesis of chiral sulfoxides. Recently, Fontecave and co-workers<sup>48</sup> have established that H<sub>2</sub>O<sub>2</sub>-dependent oxidations catalyzed by non-heme diiron complexes can proceed through metal-based pathways and can thus be made stereoselective. The synthesis of chiral oxoiron complexes and their use in the synthesis of chiral sulfoxides will be taken up in the future.

**Acknowledgment.** We thank Prof. C. Srinivasan for reading the manuscript, offering valuable suggestions, giving constant encouragement, and showing his interest in this work. We thank Prof. S. Umamathy, Department of Inorganic and Physical Chemistry, Indian Institute of Science, Bangalore, and Prof. J. Subramanian and Prof. Sambasiva Rao, Department of Chemistry, Pondicherry University, Pondicherry, for their help with the RR and EPR measurements. S.R. thanks the CSIR and UGC-DRS program for financial support, and R.R. acknowledges the partial financial

(72) Oglario, F.; Filatov, M.; Shaik, S. *Eur. J. Inorg. Chem.* **2000**, 2455.

(73) Marcus, R. A. *J. Phys. Chem. A* **1997**, *101*, 4072.



support from the DST. V.K.S. and M.G. thank the University Grants Commission, New Delhi, for selecting them to do research under the Faculty Improvement Program (FIP) and the management and principal of Vivekananda College, Tiruvedakam West, for providing FIP study leave. We also thank Prof. K. Pitchumani and Dr. R. Sevel for their help with the product analysis.

**Supporting Information Available:** EPR spectra of complex **III**d and its oxo form in CH<sub>3</sub>CN, Hammett plot

of  $E_{1/2}$  vs  $2\sigma$  values of complexes **III**a–**III**d, plots of  $1/k_1$  vs  $1/[\text{sulfide}]$  for the oxidation of *p*-XC<sub>6</sub>H<sub>4</sub>SMe with **IV**b, Hammett plot for the oxidation of *p*-acetylphenyl methyl sulfide by oxo(salen)iron complexes **IV**a–**IV**d, and plots of log  $k$  values for the reaction of oxo(salen)iron complexes **IV**a–**IV**d with sulfides against the oxidation potential of sulfides,  $E_{\text{ox}}$ . This material is available free of charge via the Internet at <http://pubs.acs.org>.

JO0108780